Available online at www.sciencedirect.com
SCIENCE DIRECT®
Journal of Nuclear Materials 319 (2003) 74–80
journal of nuclear materials
www.elsevier.com/locate/jnucmat

# Radiation-induced defect clusters in fully stabilized zirconia irradiated with ions and/or electrons

K. Yasuda [a,*], C. Kinoshita [a], S. Matsumura [a], A.I. Ryazanov [b]

[a] *Department of Applied Quantum Physics and Nuclear Engineering, Kyushu University, Hakozaki 6-10-1, Fukuoka 812-8581, Japan*
[b] *Russian Research Centre 'Kurchatov Institute', 123182 Moscow, Russia*

**Abstract**

Microstructure evolution of yttria-stabilized cubic zirconia (YSZ), $ZrO_2$–13 mol% $Y_2O_3$, was investigated through transmission electron microscopy under irradiation with electrons and/or ions. Anomalous formation of large defect clusters was found under electron irradiation subsequent to ion irradiation, such as 300 keV $O^+$, 100 keV $He^+$ and 4 keV $Ar^+$ ions. Such defect clusters were not formed solely with ion irradiation. The extended defect clusters possess strong black/black lobes contrast, and are observed preferentially around a focused electron beam at or near dislocations at temperature less than 520 K. The defect clusters were transformed into dislocation network when they reached a critical diameter of about 1.0–1.5 μm, and processes of nucleation, growth and transformation were repeated under electron irradiation. The defect clusters are assumed to be oxygen platelets induced through selective displacements of oxygen ions in YSZ with electron irradiation. An important role of the accumulation of electric charges due to the selective displacements in YSZ is also discussed.


## 1. Introduction

Extensive researches have been made toward the development of inert matrix fuels (IMFs) to utilize and burn excess plutonium in light water reactors (LWRs) generated from spent $UO_2$ fuels in LWRs and nuclear weapons [1]. Rock-like oxide fuels (ROX: multi-phase ceramics consist of yttria-stabilized cubic zirconia (YSZ), alpha-alumina and magnesium aluminate spinel) [2,3] and cermet fuels (a metal–ceramic composite in which YSZ particles are embedded in zirconium alloys, stainless steel, and other metals) [4,5] have potentials as forms for IMFs. In both forms, YSZ is the most probable candidate for a fuel phase, which contains plutonium.

Recent radiation studies revealed that YSZ is exceptionally resistant to radiations with fast neutrons and energetic ions, especially to amorphization [6–9] and volumetric swelling [10–12]. Under the radiation in pile, zirconia based IMF is exposed to a wide variety of radiation, such as by fast neutrons, fission products, electrons, gamma rays and alpha-particles, including self-irradiation from actinides with a wide range of energies up to ~100 MeV. Those radiations induce simultaneously primary radiation damage processes of displacement cascades, isolated Frenkel defects, electronic excitation, and so on, to evolve microstructure changes. Recent radiation damage studies have shown that the formation process and the stability of radiation-induced defects in some ionic and covalent ceramics are highly sensitive to ionizing radiation and/or subthreshold displacement damage [13–16]. Under such radiation environment, enhanced migration of point defects and the dissolution of defect clusters have been observed. It is, therefore, worthwhile to investigate the effects of 'soft' spectrum radiations, or electronic excitation and low energy recoil radiation, for the understanding of the nucleation-and-growth process of defect clusters in YSZ.

In the present paper, microstructure change in YSZ irradiated with energetic ions and/or electrons is

* Corresponding author. Tel.: +81-92 642 3773; fax: +81-92 642 3771.
*E-mail address:* yasudak@nucl.kyushu-u.ac.jp (K. Yasuda).

0022-3115/03/$ - see front matter © 2003 Elsevier Science B.V. All rights reserved.
doi:10.1016/S0022-3115(03)00136-3

reported. Anomalous formation of large defect clusters is shown under electron irradiation subsequent to ion irradiation. The characteristic features and formation process of the defect clusters are described, and the role of 'soft' radiation spectrum on the radiation damage process of YSZ is discussed.

## 2. Experimental details

A rod of man-made single crystal of fully stabilized cubic zirconia from Earth Jewelry Co., which contains 13 mol% $Y_2O_3$ (YSZ), was used in the present study. The crystal was aligned nearly to a <1 1 1> orientation and cut into plates with 0.5 mm thickness followed by mechanical shaping to transmission electron microscopy (TEM) disk-specimens with 3.0 mm in diameter and 0.12 mm in thickness. Wedge-shaped electron transparent specimens were prepared by dimpling and $Ar^+$-ion thinning processes from the disk specimens. A part of the specimens was annealed in air at 1670 K for 7.2 ks to eliminate defects, which were induced during ion-thinning process. Those specimens were irradiated with 300 keV $O^+$ ions at 470 K to $O^+$ fluences of $5.1 \times 10^{17}$–$5.1 \times 10^{18}$ $m^{-2}$ with an $O^+$ flux of $2.5 \times 10^{16}$ $m^{-2}\,s^{-1}$, or with 100 keV $He^+$ ions at 870 K to a $He^+$ fluence of $1.0 \times 10^{20}$ $m^{-2}$ with a $He^+$ flux of $3.0 \times 10^{16}$ $m^{-2}\,s^{-1}$. Ion-irradiation of 300 keV $O^+$ ions and 100 keV $He^+$ ions were respectively performed in a TEM-accelerator facility at Takasaki Ion Accelerators for Advanced Radiation Application (TIARA) in Japan Atomic Energy Research Institute (JAERI) and in a disktron-type ion accelerator at Kyushu University. The Monte Carlo simulation of SRIM-2000 [17] revealed that most of 300 keV $O^+$ ions and 100 keV $He^+$ ions penetrate the specimens at thicknesses less than ~200 nm, where TEM observations were performed in the present study. A value of 40 eV was used as mean displacement energy for Zr and O ions of YSZ for the calculation. The displacement damage rates yield by 300 keV $O^+$ and 100 keV $He^+$ ions were estimated to be $1.2 \times 10^{-3}$ and $1.1 \times 10^{-4}$ dpa $s^{-1}$, respectively at a depth of 200 nm with each ion flux described above. These ion-irradiated specimens were subjected to electron irradiation with energies from 100 to 1000 keV at temperatures from 370 to 600 K in a High Voltage Electron Microscope (JEM-1000, JEOL Co. at HVEM Laboratory of Kyushu University) and TEM-accelerator facility (JEM-4000EX, JEOL Co. at TIARA in JAERI). The electron irradiations were performed with a focused beam with a beam diameter of around 1–2 μm. The electron flux at the center of the focused electron beam was around $10^{23}$ $m^{-2}\,s^{-1}$. Microstructure change was recorded in situ in TEMs during electron irradiation either on films or through a video system.

## 3. Results and discussion

Fig. 1 shows a typical example of bright-field (BF) images of defect clusters in YSZ irradiated with 300 keV $O^+$ ions at 470 K at an $O^+$ fluence of $5.1 \times 10^{17}$ $m^{-2}$, corresponding to $2.5 \times 10^{-2}$ dpa at a thickness of 200 nm, followed by irradiation with a focused 200 keV electron beam at 370 K. Defect clusters with strong black/black lobes contrast are formed with size up to ~300 nm in diameter, preferentially around the focused electron beam. This indicates that there exists strong and long-range stain field around the defect clusters. It is important to emphasize here that these defect clusters were not observed in YSZ irradiated solely with 300 keV $O^+$ ions at 470 K up to an $O^+$ fluence of $5.0 \times 10^{18}$ $m^{-2}$, and that they were observed after subsequent electron irradiation with a focused electron beam. Analogous defect cluster formation was observed in specimens irradiated at 470 K with a 200 keV electron beam subsequent to 100 keV $He^+$ ions at 870 K at a dose of 0.6 dpa. Similar to the microstructure observed with 300 keV $O^+$ ions, no extended defect clusters, except tiny dot contrast features, were observed in specimens when irradiated solely with 100 keV $He^+$ ions.

Fig. 2(a)–(d) shows microstructure in YSZ irradiated by a focused electron beam at 470 K with different energies ranging from 100 to 1000 keV. Ion irradiation was performed with 300 keV $O^+$ ions at 470 K ((a)–(c)) or 4 keV $Ar^+$ ions at ambient temperature (d) prior to

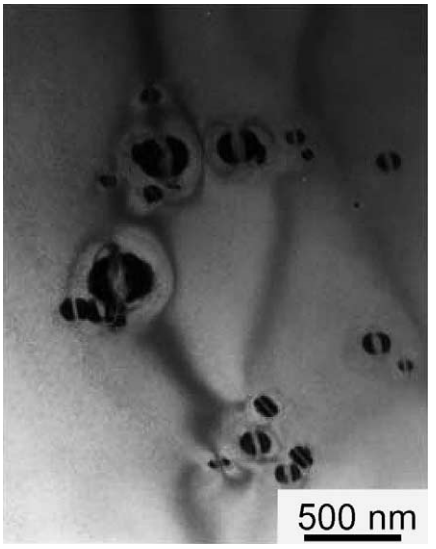


Fig. 1. Extended defect clusters formed in YSZ around a 200 keV focused electron beam of 200 keV with a beam diameter of ~1 μm. The specimen was irradiated at 470 K with 300 keV $O^+$ ions to $5.1 \times 10^{17}$ $m^{-2}$ followed by 200 keV electrons at 370 K for 210 s with an $e^-$ flux of $1.3 \times 10^{23}$ $m^{-2}\,s^{-1}$. The focused electron beam was illuminated around the center of the photo.

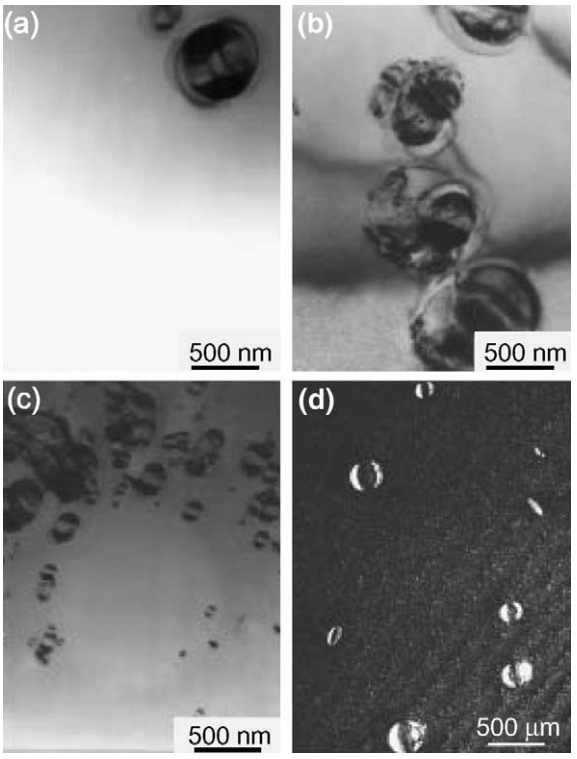


Fig. 2. Electron-energy dependent microstructure of YSZ irradiated with a focused electron beam subsequent to irradiation with ions under bright-field conditions (a)–(c) and a dark-field condition (d). Irradiation conditions are: (a) 100 keV electrons at 470 K and 300 keV $O^+$ ions at 470 K, (b) 200 keV electrons at 470 K and 300 keV $O^+$ ions at 470 K, (c) 400 keV electrons at 470 K and 300 keV $O^+$ ions at 470 K, and (d) 1000 keV electrons at 470 K and 4 keV $Ar^+$ ions at 300 K.

electron irradiation. Large defect clusters are seen in Fig. 2 at all electron energies from 100 to 1000 keV, although irradiation conditions, that is, ion species, energy and irradiation temperature, are different from each micrographs. It should be noticed that low energy electrons, such as 100 and 200 keV, induce the defect clusters in YSZ. Further interesting feature is that these defect clusters were preferentially formed in thick regions of specimens. This indicates that the defect clusters are not formed through a surface dominant process but through a process occurred in the bulk of the specimen.

Fig. 3 shows temperature dependence for the formation of defect clusters. Large defect clusters as shown in Figs. 1 and 2 were observed at temperatures of 470 K (Fig. 3(a)) under 200 keV electron irradiation subsequent to 300 keV $O^+$ ion irradiation at 470 K. However, no nucleation of the defect clusters was observed under 200 keV electron irradiation at temperature higher than 520 K (Fig. 3(b)), whereas the defect clusters formed below 520 K grew at higher temperatures than 520 K.

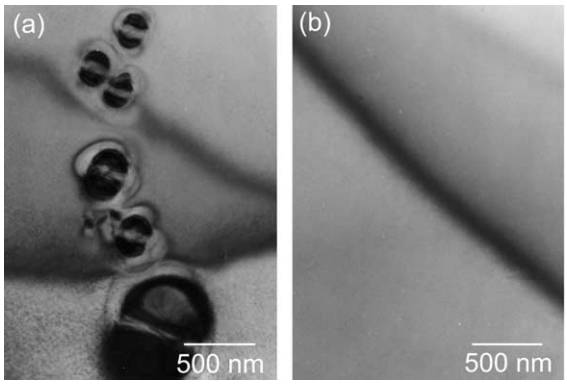


Fig. 3. Bright-field images in YSZ irradiated with 200 keV focused electron beam subsequent to ion irradiation with 300 keV $O^+$ ions at 470 K at an $O^+$ dose of $5.1 \times 10^{17}$ $m^{-2}$ at electron irradiation temperature of 470 K (a) and 520 K (b). No formation of defect clusters was observed at 520 K and higher temperature.

The nucleation regime of the defect clusters is, therefore, less than 520 K, and it suggests that the mobility of the point defects included in the defect clusters, which will be discussed later to be oxygen interstitials, is very high.

A sequence of the growth process of the defect cluster is shown in Fig. 4 at 470 K under 200 keV electron irradiation. Ion-irradiation condition is equivalent to that of Fig. 1, and the flux of electron beam was estimated to be $\sim 5 \times 10^{21}$ $m^{-2}\,s^{-1}$ (electron beam was not focused during the record of the growth process through the video system). Fig. 4 shows that the defect cluster grows with increasing irradiation time, accompanying strong black/black lobes contrast ((a)–(d)). The growth rate of the defect cluster was estimated to be $\sim 1$ $nm\,s^{-1}$ from the growth process of the defect (from (a) to (d)), illustrating the very fast growth rate. At micrograph (d), the defect contrast is seen to change from black/black lobes to dislocation networks in a very short time ((d)–(e)). Several segments of dislocations are generated after the transformation (e), and continuous electron irradiation induces new several defect clusters possessing the analogous contrast to (a), preferentially at or near dislocation lines (a few examples are indicated by triangles in (f)). These new defect clusters are seen to grow with electron irradiation. An interesting feature of the growth process of the newly induced defect clusters is that they are again transformed to dislocation lines after the growth process, as one example is indicated by triangle in (h) and (i). Namely, the defect cluster is found to repeat the growth, transformation from black/black lobes to dislocation lines, and re-nucleation processes under electron irradiation in an originally formed defect cluster. The critical diameter for the transformation was around 1.0–1.5 μm if the defect clusters exist rather separately from other defect clusters. In the case where a

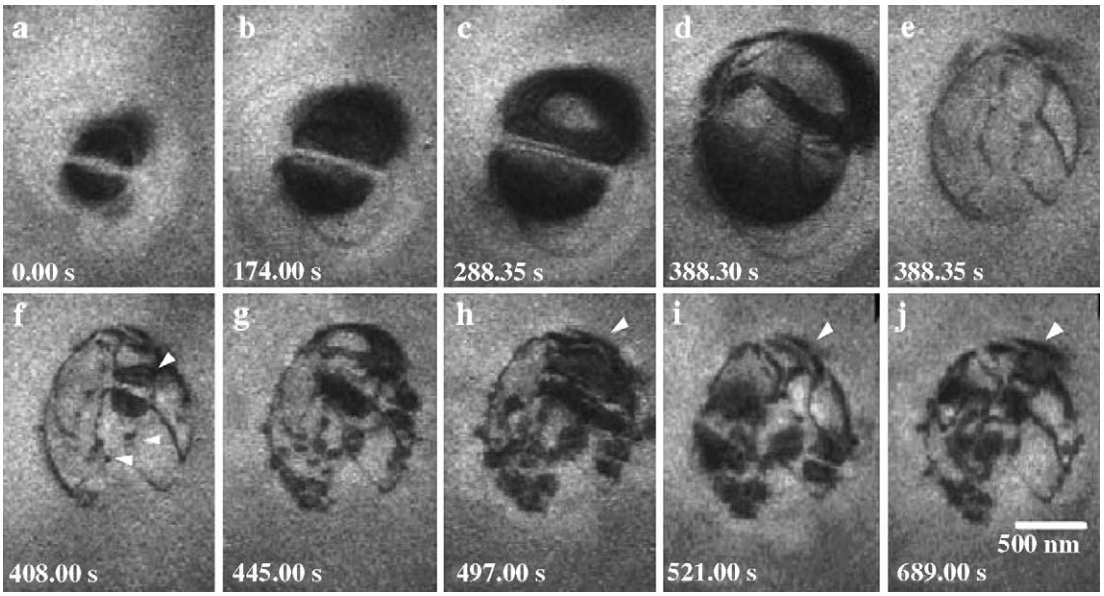


Fig. 4. Growth process of a defect cluster in YSZ under 200 keV electron irradiation at 470 K with an electron flux of $\sim 5 \times 10^{21}$ $m^{-2}$ $s^{-1}$. The specimen was irradiated originally with 300 keV $O^+$ ions at 470 K at an $O^+$ fluence of $5.1 \times 10^{17}$ $m^{-2}$ followed by a focused electron beam (electron flux at the center of the beam was $\sim 10^{23}$ $m^{-2}$ $s^{-1}$) at 470 K to nucleate the defect cluster. Real electron-irradiation time from the microstructure of (a) is shown at each photo. The diffraction vector is $g = 220$.

defect cluster exists in the vicinity of other defect clusters, the critical size is smaller (an example is seen in Fig. 5(h) and (i)).

In order to analyze the nature of the defect clusters, their diffraction contrast was taken with different diffraction vectors of <2 2 0> system using an incident electron beam closed to a $[\bar{1}\,1\,1]$ direction, and BF images of the defect clusters in a same area are shown in Fig. 5. The contrast-free line of the defects is seen mostly perpendicular to the corresponding diffraction vector for three different 220 vectors, indicating that the strain field around the defect clusters is isotropic on the $(\bar{1}\,1\,1)$ plane. This implies that the defect clusters are not the normal interstitial-type dislocation loops, as it is also

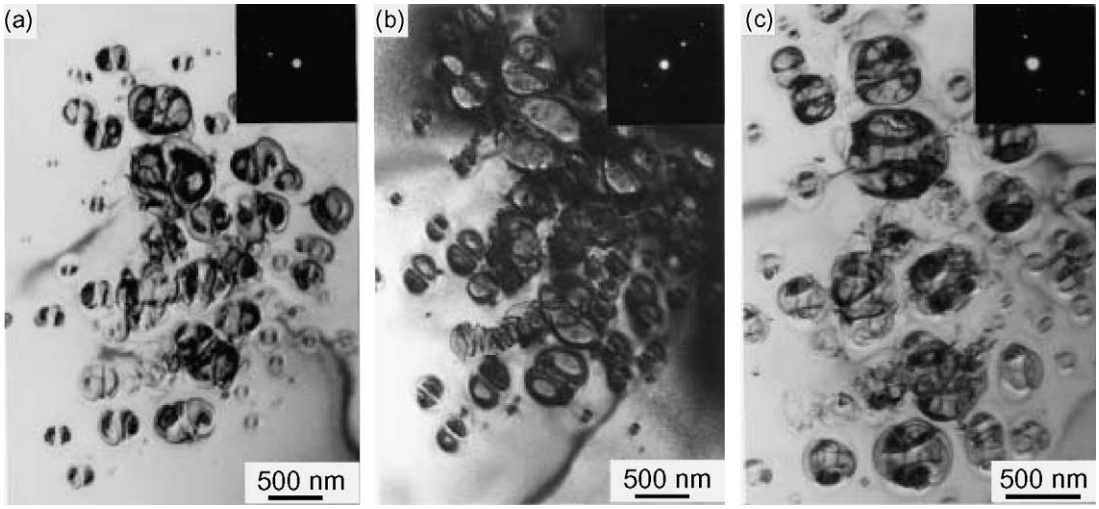


Fig. 5. BF images of the defect clusters of YSZ taken with three different diffraction vectors of (a) $\bar{2}\bar{2}0$, (b) $0\bar{2}\bar{2}$ and (c) $\bar{2}0\bar{2}$ at the same area. The incident electron beam is from nearly a $[\bar{1}\,1\,1]$ direction. The larger size in the defect clusters observed in (c) than in (a) is due to the rapid growth of the defect clusters during photos record.

suggested by the difference in BF images of dislocation loops in previously reported ion-irradiated YSZ [6,7].

The observed defect clusters in YSZ shown in Figs. 1–4 are analogous to those reported by Baufeld et al. [18] and Gomez-García et al. [19,20], in which similar black/black lobes contrast is observed under electron-beam irradiation in fully stabilized zirconia with a nominal concentration of 9.4 mol% $Y_2O_3$. Baufeld et al. irradiated YSZ with 1000 keV electrons at room temperature and 473 K, and observed the defect clusters preferentially along dislocations that were induced by high temperature compression test prior to electron irradiation. They concluded that the defect clusters are prismatic dislocation loops of interstitial nature with a character of $a/3\langle 1\,1\,1\rangle\{1\,1\,1\}$, and that the defect formation is induced by aggregation of interstitials induced through displacement damage with 1000 keV electrons. Gomez-García et al., on the other hand, concluded that the defect clusters are ZrN precipitates (a large amount of dissolved nitrogen was found in their YSZ crystal [21]) induced by beam heating effects, since the defect clusters were induced with a wide range of electron energies from 100 to 1500 keV.

Electron-beam induced displacement cross-sections through elastic collision process, which is through Oen's table based on Bethe's formula [22,23], are shown in Fig. 6 for Zr- and O-sublattice. Since no reported values are available in the literature for the displacement energy in YSZ, we referred a typical mean value assumed for zirconia and pyrochlore (40 eV for Zr- and O-sublattice) [9,24], and a reported value of $UO_2$ (40 eV for U-sublattice, 20 eV for O-sublattice) having same $CaF_2$ crystal structure [25]. The results of cross sections are, therefore,

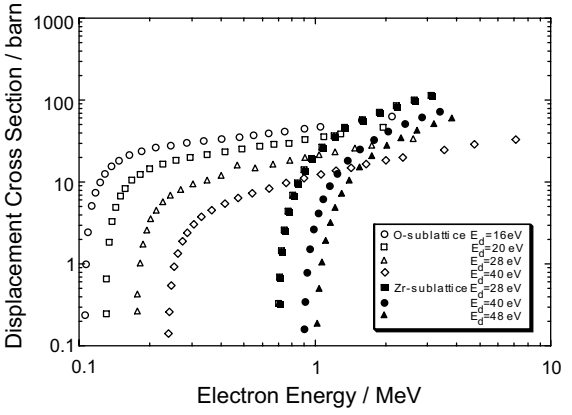


Fig. 6. Calculated displacements cross-section for Zr- and O-sublattice in zirconia using Bethe's formula [16] as a function of electron energy. Values in Fig. 5 are from Oen's Table [17]. Cross section is plotted with displacement energies of 28–48 eV for Zr sublattice and 16–40 eV for O sublattice. The cross section of Y ions is almost same with that of Zr ions due to the close mass of the element.

plotted with a band of displacement energies of 28–48 eV for Zr-sublattice and 16–40 eV for O-sublattice. Fig. 6 clearly illustrates that electrons with energy less than 900 keV hardly displace Zr-sublattice in YSZ, whereas O-sublattice can be displaced with electrons around 100–200 keV. A value of $10^{-5}$–$10^{-4}$ dpa $s^{-1}$ is obtained by using the cross sections in Fig. 6 as an elastic displacement rate for O-sublattice with a focused 200 keV electron beam at a flux of $10^{23}$ $m^{-2}\,s^{-1}$. This indicates that electron irradiation in the present study is a selective displacement damage condition for O-sublattice in YSZ. However, it seems to be difficult to explain the very high growth rate of the defect clusters, approximately 1 nm $s^{-1}$ with an electron flux of $5 \times 10^{21}$ $m^{-2}\,s^{-1}$, solely through the corresponding elastic displacement rate, or $\sim 10^{-6}$ dpa $s^{-1}$. This suggests a possibility of displacements of oxygen ions through an electronic excitation process, as previously reported for anion sublattice in halides and $SiO_2$ [26–28], although there have been no reports to reveal such electronic excitation-induced displacements in cubic zirconia.

On the basis of the discussion above, the most probable explanation for the defect clusters is oxygen clusters, induced by aggregation of selectively displaced oxygen ions with electron irradiation. Taking the specimen thickness (around 200 nm or less) and the diameter of the defect clusters (more than 1.0 μm in diameter) into consideration, the defect clusters are not spherical but probably are coherent platelets lying on $\{1\,1\,1\}$ planes. The defect clusters are, therefore, considered to possess strong strain contrast as shown in Figs. 1–5. As a support of this speculation, a theoretical calculation of YSZ has revealed that much stronger stress and strain fields are induced around a charged oxygen platelet than a neutral dislocation loop [29]. An electric field induced by the accumulated charge in the defect clusters (oxygen platelet) causes additional stress and strain fields around the charged oxygen platelet, depending on the effective charge of oxygen interstitials in the clusters. The induced stress with the critical size of $\sim$1.0 μm has revealed nearly the equivalent stress to generate dislocations in YSZ [30].

It should be noted here that the defect clusters were also formed solely with electron irradiation (without preceding ion irradiation) when a higher flux of electron beam was illuminated at thicker regions of the specimen. In other words, the preceding ion irradiation is not absolutely necessary to induce the defect clusters in YSZ. The ion irradiation is, therefore, considered to induce dot-contrast defects and/or 'invisible' defects, which act as nucleation sites of the defect clusters formed under electron irradiation. Namely, ion irradiation is considered to play an equivalent role with preexisting dislocation lines, where the defect clusters were preferentially nucleated as shown in Fig. 4 and in Refs. [18,20]. A difference on the radiation damage process between ion-

and electron-irradiation is that electrons induce displacements only in oxygen ions whereas ion irradiation induces them for both ions. The ratio of displacement rate for Zr ions to O ions with 300 keV $O^+$ ion and 100 keV $He^+$ ion are evaluated respectively through SRIM-2000 [17] to be 0.66 and 0.71 with an assumption of $E_d = 40$ eV for both Zr and O ions, and 0.30 and 0.34 with $E_d = 40$ eV for Zr and 20 eV for O ions. The selective displacement damage conditions are, at this moment, considered to influence the nucleation-and-growth process of the anomalous defect clusters observed under electron irradiation in YSZ.

The focused electron beam used in the present study not only causes a high flux of electrons but also a concentration gradient of displaced oxygen ions inside the electron beam. Such concentration gradient induces the migration of interstitials from the center toward the outside of the beam, and therefore the defect clusters are considered to be formed preferentially around the focused electron beam.

## 4. Summary and conclusions

Electron-beam irradiation subsequent to ion irradiation has been found to induce anomalous large defect clusters in yttria-stabilized cubic zirconia (YSZ). These defect clusters possess strong strain field, rapid growth rate ($\sim$1 nm $s^{-1}$ under 200 keV electron irradiation at a flux of $5 \times 10^{23}$ $m^{-2}$ $s^{-1}$), and are induced around the focused electron beam preferentially at or near dislocation networks and tiny dot-contrast defects. The defect clusters are transformed from black/black lobes contrast to dislocation networks when they reach a critical diameter of 1.0–1.5 μm. Processes of nucleation, growth and transformation of the defect clusters are repeated under electron irradiation. A most probable explanation for the defect cluster is the oxygen platelets, which are formed due to the selective displacement of oxygen sublattice in YSZ. The physical mechanism for the selective displacement damage, that is, either elastic or inelastic process, has not been clarified in the present study. However, the present results suggest an important role of low energy recoils and/or electronic excitation for the radiation damage processes in YSZ, which induce selective radiation damage in the oxygen sublattice of YSZ. Another important feature of the damage process is that the defect clusters generate dislocations through the transformation at a critical diameter, and multiply the defect clusters at and near the generated dislocations.

## Acknowledgements

All the irradiations and TEM experiments were carried out in the HVEM Laboratory, Kyushu University and in TIARA at JAERI. We are grateful to M. Kutsuwada and E. Tanaka at Kyushu University and H. Abe at University of Tokyo for their technical assistance to operate ion accelerators and TEMs. This work was supported in part by Japan Nuclear Cycle Development Institute (JNC) and TEPCO research foundation.

## References

[1] C. Degueldre, J.M. Paratte, J. Nucl. Mater. 274 (1999) 1.
[2] H. Akie, T. Muromura, H. Takano, S. Matsuura, Nucl. Technol. 107 (1994) 182.
[3] N. Nitani, K. Kuramoto, T. Yamashita, Y. Nihei, Y. Kimura, these Proceedings. doi:10.1016/S0022-3115(03)00140-5.
[4] A. Fernandez, R.J.M. Konings, J. Somers, these Proceedings. doi:10.1016/S0022-3115(03)00132-6.
[5] M.A. Pouchon, M. Nakamura, C. Hellwig, F. Ingold, C. Degueldre, these Proceedings. doi:10.1016/S0022-3115(03)00131-4.
[6] K. Yasuda, M. Nastasi, K.E. Sickafus, C.J. Maggiore, N. Yu, Nucl. Instrum. and Meth. B 136–138 (1998) 499.
[7] K.E. Sickafus, Hj. Matzke, K. Yasuda, P. Chodak III, R.A. Verrall, G.P. Lucutta, R.H. Andrew, A. Toros, R. Fromknecht, N.P. Baker, Nucl. Instrum. and Meth. B 141 (1998) 358.
[8] K.E. Sickafus, Hj. Matzke, Th. Hartmann, K. Yasuda, J.A. Valdez, P. Chodak III, M. Nastasi, R.A. Verrall, J. Nucl. Mater. 274 (1999) 66.
[9] L.M. Wang, S.X. Wang, S. Zhu, R.C. Ewing, J. Nucl. Mater. 289 (2001) 122.
[10] N. Sasajima, T. Matui, K. Hojou, S. Furuno, H. Otsu, K. Izui, K. Murumura, Nucl. Instrum. and Meth. B 141 (1998) 487.
[11] C. Degueldre, P. Heimgartner, G. Ledergerber, N. Sasajima, K. Hojou, T. Muromura, L.M. Wang, R. Gong, R. Ewing, Mater. Res. Soc. Symp. Proc. 439 (1997) 625.
[12] N. Sasajima, T. Matui, S. Furuno, T. Shiratori, K. Hojou, Nucl. Instrum. and Meth. B 166&167 (2000) 250.
[13] S.J. Zinkle, J. Nucl. Mater. 219 (1995) 113.
[14] K. Yasuda, C. Kinoshita, R. Morisaki, H. Abe, Philos. Mag. A 78 (1998) 583.
[15] K. Yasuda, C. Kinoshita, Nucl. Instrum. and Meth. B 191 (2002) 559.
[16] K. Yasuda, C. Kinoshita, S. Matsumura, Defect Diffus. Forum 206&207 (2002) 53.
[17] J.F. Ziegler, J.P. Biersack, U. Littmark, The Stopping and Range of Ions Solids, Pergamon, New York, 1985.
[18] B. Baufeld, D. Baither, U. Messerschmidt, M. Bartsch, I. Merk, J. Am. Ceram. 76 (1993) 3163.
[19] D. Gozez-García, J. Martínez-Fernández, A. Domínguez-Rodriguez, Philos. Mag. Lett. 81 (2001) 173.
[20] D. Gozez-García, J. Martínez-Fernández, A. Domínguez-Rodriguez, K.H. Westmacott, J. Am. Ceram. Soc. 79 (1996) 2733.
[21] D. Gozez-García, J. Martínez-Fernández, A. Domínguez-Rodriguez, K.H. Westmacott, J. Am. Ceram. Soc. 79 (1996) 487.
[22] O.S. Oen, Cross section for atomic displacements in solids by fast neutrons, ORNL 4873 (1973).

[23] H. Bethe, J. Ashkin, in: E. Segre (Ed.), Experimental Physics, vol. 1, Wiley, New York, 1953, p. 166.
[24] S. Zhu, X.T. Zu, L.M. Wang, R.C. Ewing, Appl. Phys. Lett. 80 (2001) 4327.
[25] F.W. Clinard Jr., L.W. Hobbs, in: R.A. Johnson (Ed.), Physics of Radiation Effects in Crystals, Elsevier Science, Amsterdam, 1986, p. 392.
[26] L.W. Hobbs, M.R. Pasucci, J. de Phys 41 (1980) 236.
[27] M.L. Knotek, Rep. Prog. Phys. 47 (1984) 1499.
[28] G.S. Chen, C.B. Boothroyd, C.J. Hamphreys, Philos. Mag. A (1998) 491.
[29] A.I. Ryazanov, K. Yasuda, C. Kinoshita, A.V. Klaptsov, J. Nucl. Mater. 307–311 (2002) 918.
[30] A.I. Ryazanov, K.Yasuda, C. Kinoshita, A.V. Klaptsov, J. Nucl. Mater., in preparation.